State Dependence of Atmospheric Response to Extratropical North Pacific SST Anomalies

GUIDI ZHOU[a]

GEOMAR Helmholtz Centre for Ocean Research Kiel, Kiel, Germany

MOJIB LATIF AND RICHARD J. GREATBATCH

GEOMAR Helmholtz Centre for Ocean Research Kiel, and Cluster of Excellence "The Future Ocean," University of Kiel, Kiel, Germany

WONSUN PARK

GEOMAR Helmholtz Centre for Ocean Research Kiel, Kiel, Germany

(Manuscript received 22 September 2015, in final form 27 September 2016)

ABSTRACT

By performing two sets of high-resolution atmospheric general circulation model (AGCM) experiments, the authors find that the atmospheric response to a sea surface temperature (SST) anomaly in the extratropical North Pacific is sensitive to decadal variations of the background SST on which the SST anomaly is superimposed. The response in the first set of experiments, in which the SST anomaly is superimposed on the observed daily SST of 1981–90, strongly differs from the response in the second experiment, in which the same SST anomaly is superimposed on the observed daily SST of 1991–2000. The atmospheric response over the North Pacific during 1981–90 is eddy mediated, equivalent barotropic, and concentrated in the east. In contrast, the atmospheric response during 1991–2000 is weaker and strongest in the west. The results are discussed in terms of Rossby wave dynamics, with the proposed primary wave source switching from baroclinic eddy vorticity forcing over the eastern North Pacific in 1981–90 to mean-flow divergence over the western North Pacific in 1991–2000. The wave source changes are linked to the decadal reduction of daily SST variability over the eastern North Pacific and strengthening of the Oyashio Extension front over the western North Pacific. Thus, both daily and frontal aspects of the background SST variability in determining the atmospheric response to extratropical North Pacific SST anomalies are emphasized by these AGCM experiments.

1. Introduction

It is universally believed that extratropical sea surface temperature (SST) anomalies are largely forced by the atmosphere on interannual to decadal time scales, as put forward by the pioneering work of Bjerknes (1964) and confirmed by many succeeding studies (e.g., Cayan 1992a,b,c). On the other hand, Bjerknes (1964) also proposed that on longer time scales, the ocean significantly contributes to the extratropical SST variability, an argument supported subsequently by, for example, Deser and Blackmon (1993), Kushnir (1994), Nakamura et al. (1997), and Gulev et al. (2013). However, there is a controversy about whether extratropical SST anomalies significantly affect the large-scale atmospheric circulation, and if so, how. Unlike in the tropics where a pronounced locally driven, thermally direct, and far-reaching atmospheric response to SST changes is found, owing to deep convection (Neelin et al. 1998), the extratropical response to SST anomalies is in most cases smaller than the intrinsic atmospheric variability (Kushnir et al. 2002). Thus, more effort is required to tackle the low signal-to-noise ratio problem.

Over the last three decades or so, considerable effort has been applied to this problem by means of observational analyses (Liu et al. 2006; Frankignoul and

[a] Current affiliation: Max Planck Institute for Meteorology, Hamburg, Germany.

Corresponding author e-mail: Dr. Guidi Zhou, guidi.zhou@mpimet.mpg.de

DOI: 10.1175/JCLI-D-15-0672.1

Sennéchael 2007; Wen et al. 2010; Liu et al. 2012a,b), theoretical studies (e.g., Frankignoul 1985), forced atmospheric general circulation model (AGCM) experiments (Palmer and Sun 1985; Latif and Barnett 1994; Kushnir and Held 1996; Peng et al. 1997; Liu and Wu 2004), and coupled climate model simulations (Latif and Barnett 1994, 1996; Saravanan 1998; Liu and Wu 2004; Kwon and Deser 2007; Liu et al. 2007; Lee et al. 2008; Zhong and Liu 2008). The atmospheric response to extratropical SST anomalies is still controversial and sometimes perplexing, yet a set of common conclusions has been widely accepted (see Kushnir et al. 2002). Among other things, the response can be modulated by baroclinic eddy feedback, and it can depend on the atmospheric background state (e.g., Peng et al. 1995; Ting and Peng 1995; Peng et al. 1997; Peng and Whitaker 1999; Brayshaw et al. 2008; Taguchi et al. 2012). Regarding the mechanism by which the atmospheric background state can affect the atmospheric response, Brayshaw et al. (2008) performed idealized aquaplanet experiments under perpetual equinox conditions and provided a preliminary explanation in terms of the relative latitudinal position of the subtropical jet and the meridional SST gradient change. However, the current understanding of the state dependence of the atmospheric response to extratropical SST anomalies is still far from satisfactory.

Further, although the atmospheric background state can be ultimately determined by the background SST to a great extent in forced AGCM simulations, the role of the background SST variability, on which an SST anomaly is superimposed, has received little attention. Observational studies have been devoted to detecting the response and describing its characteristics, whereas model experiments usually employ climatologically varying background SST, which is unrealistic given the large daily and interannual SST variability in the extratropics. Recently, Zhou et al. (2015, hereafter Z15) show that daily variability in the background SST can be important for determining the atmospheric response to midlatitude North Pacific SST anomalies. Many recent studies (e.g., Minobe et al. 2008; Taguchi et al. 2009; Smirnov et al. 2015) have also pointed out the potential importance of the sharp subpolar SST fronts associated with the western boundary currents. Finally, small-scale air–sea interactions linked to mesoscale ocean eddies over the North Pacific in the Kuroshio Extension region have been identified as a major factor in regulating large-scale climate conditions in that area (Ma et al. 2016).

Here, we follow up the work of Z15. We investigate the state dependence of the atmospheric response to midlatitude North Pacific SST anomalies by superimposing them on the observed daily SST during 1981–2000, which exhibits significant decadal variability. Section 2 briefly introduces the model and experimental setup as well as the forcing SSTs. In section 3, we examine the characteristics, mechanism, and decadal evolution of the response. The possible role of the background atmospheric state is discussed in section 4 and the role of the background SST in section 5. We argue that the reason for the difference in the decadal-mean response is linked to the decadal background SST changes, in particular, changes in the daily SST variability and the Oyashio Extension front. Summary and discussion are presented in section 6.

2. Model, experimental setup, and data

We carry out a series of SST-forced simulations with the ECHAM5 atmospheric general circulation model (AGCM; Roeckner et al. 2003) on a T213 grid (~60 km × ~60 km) with 31 vertical levels extending up to 10 hPa, resolving only the lower part of the stratosphere. Li (2006, Table 4.3) showed that a 20-yr Atmospheric Model Intercomparison Project (AMIP)-type (Gates et al. 1999) run with the same model simulates the planetary wave climatology reasonably well, in some aspects even better than a high-top (0.01 hPa) version of the model.

The SST data used in this study cover the period 1981–2000 and are from the daily NOAA OISST dataset (Reynolds et al. 2007), and the data have been linearly interpolated from the original ¼° resolution to the T213 resolution of the AGCM. To examine the atmospheric response to large-scale decadal North Pacific SST anomalies, we first compute the Pacific decadal oscillation (PDO; Mantua et al. 1997) index as the leading principal component (PC) of winter (DJF) mean North Pacific (20°–60°N, 120°E–100°W) SSTs. The ENSO signature was reduced in the SSTs in advance by removing the variability associated with the leading two PCs of winter-mean tropical Pacific (30°S–20°N, 120°E–100°W) SSTs by means of linear regression. The multiyear time series of SSTs in October–March are then respectively regressed onto the ''ENSO removed'' winter mean PDO index, producing six patterns that are positioned at the middle of the corresponding months and then interpolated into a daily record from which only November–February are extracted. This record is used as the SST anomaly forcing in the AGCM simulations described below. We presume that such an evolving SST anomaly with a seasonal cycle is more realistic than a constant SST anomaly as used in previous studies. The SST anomaly forcing is only used in the North Pacific; no SST anomaly forcing is used outside the North Pacific.

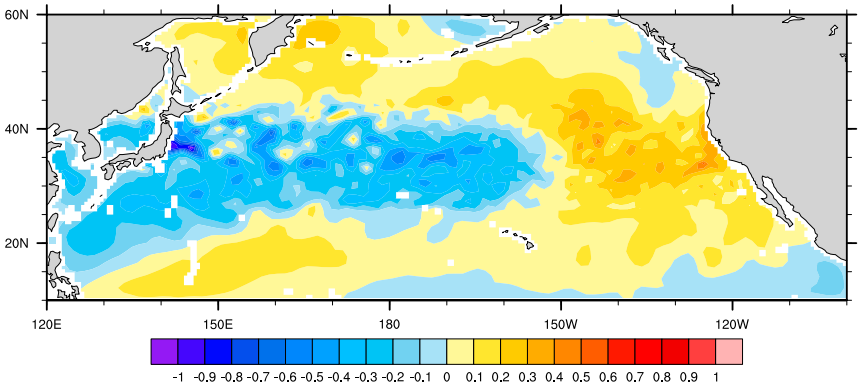

FIG. 1. Positive phase of the winter-mean (DJF) SST anomaly forcing in the North Pacific (°C). No SST anomaly is present in other basins.

Figure 1 depicts the SST anomaly pattern averaged over boreal winter (DJF).

In contrast to many previous studies using climatological monthly SST as background SST, we superimpose the SST anomalies on the observed daily SSTs during 1981–2000. Our approach appears to be more realistic, as it retains significant daily and interannual variability in the background SST. Z15 has shown that although SST variability outside the North Pacific is present, this variability is of minor importance to the extratropical atmospheric response averaged over the 1981–90 decade. We argue here that the same is also true for the 1991–2000 decade.

The model is integrated for each of the 20 winters (NDJF) during 1981–2000, with November considered as the ''spinup'' period and omitted in the subsequent analyses. Experiments are performed with both the positive and negative polarity of the SST anomalies separately, repeated for each year. The winter-mean (DJF) atmospheric response is then defined as the difference between the model runs forced by the positive and negative polarity (positive minus negative).

For the decade 1981–90 (Dec8190), the model setup is exactly the same as the daily global (DAGL) experiment in Z15, with one integration per winter, each initialized with the 1 November conditions of the corresponding year taken from a control run (CTRL) forced by observed daily SSTs of 1981–2000 but with no SST anomaly applied. For the decade 1991–2000 (Dec9100), in order to increase sample size and thus statistical significance, two integrations are performed for each winter, using the 1 November and 1 December conditions from the control run to initialize the integrations on 1 November. The average of the two integrations is used in the subsequent analyses. The Dec9100 simulation is an extension to the DAGL experiment to the 1991–2000 decade.

Although the number of realizations for each winter is small, when analyzing decadal averages, the sample size is increased to 10 (20) for Dec8190 (Dec9100). The robustness of the decadal-mean Dec8190 results is further supported by additional sensitivity experiments presented in Z15. Statistical significance of the decadal averages is estimated using a one-sample t test with 9 (19) degrees of freedom for Dec8190 (Dec9100). We note that for Dec9100, the results do not significantly change if only one of the two integrations in each winter is used to compute the decadal-mean response. Additionally, the linear trends during 1981–2000 provide useful information about decadal variability and are also tested for statistical significance with a t test using 18 degrees of freedom. More details can be found in the appendix.

3. Response

a. *Linear trend*

We examine the 500-hPa geopotential height response over the North Pacific (10°–60°N) in the western (WNP; 120°–180°E) and eastern (ENP; 180°–100°W) parts separately (Fig. 2) because the dynamics in the storm-track entrance and exit regions are different (Chang et al. 2002). The model simulates an ascending trend which is statistically significant at the 95% level over both regions: the two decadal means are negative during Dec8190, while during Dec9100, they wobble around zero. This is indicative of a decadal transition between two different response regimes. Gan and Wu (2012) showed using observations that a regime (sign) transition of the atmospheric response can indeed be found on multidecadal time scales. In the following, the two decadal-mean responses are investigated separately to obtain further insight into the role of the background SSTs in the decadal transition.

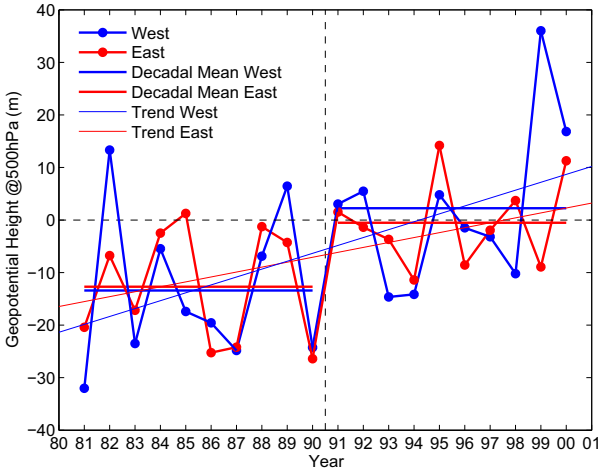

FIG. 2. Time series of 500-hPa geopotential height (m) responses during winter (DJF) averaged over the western (120°–180°E; blue curves) and eastern (180°–100°W; red curves) North Pacific (10°–60°N). The thick dotted curves show the time series, the thick horizontal lines denote the decadal means, and the thin lines are the decadal trends. The trends for the western and eastern North Pacific are both statistically significant at the 95% level, but they are not statistically different from each other.

b. *Decadal-mean response: 1981–90*

The decadal-mean atmospheric pressure response during Dec8190 (Fig. 3) is equivalent barotropic in the extratropics, as indicated by the sea level pressure (Fig. 3a) and 500-hPa geopotential height (Fig. 3b) responses as well as the zonal mean vertical section to be shown later. A significant zonal wavenumber-2 wavelike pattern is simulated in the midlatitudes, with anomalously low pressure over the Pacific and Atlantic and anomalously high pressure over North America and Eurasia. The strongest response is found over the ENP and appears to be the origin of the wave train. Correspondingly, in the positive compared to the negative polarity case (Fig. 3c), the westerly jets at 500 hPa are more zonally elongated over the oceans and terminate more abruptly over the continents. Similarly, the 500-hPa storm-track response exhibits a NW–SE shift over the ENP, which in turn makes the storm track more zonally confined (Fig. 3d). The ENP trough is associated with enhanced vertical motion at its eastern side that goes along with enhanced convective precipitation (Figs. 3e,f), related to the anomalous storm track. Over the WNP, the storm-track response is weak and insignificant. However, a region of significantly reduced vertical motion and convective rainfall over the East China Sea, compensated by upward motion to the south, is found that largely follows the regional SST anomaly pattern, suggesting a linear response to the SST anomaly in this region.

The response (i.e., the winter-mean difference between the two SST polarity cases) in the ENP conforms to an eddy-mediated response (Z15; Kushnir et al. 2002). First, the SST forcing drives an anomalous eddy vorticity flux convergence near 40°N in the upper troposphere (Fig. 4a). This leads to enhanced vorticity to the north at about 45°N, decreased geopotential height, and an accelerated jet stream, consistent with the quasigeostrophic vorticity equation (Hoskins et al. 1983). Second, the rather abrupt termination of the jet stream in the east causes increased barotropic deformation of individual propagating eddies near the storm-track exit region, feeding back positively onto the storm track (Chang et al. 2002). Anomalous convergence of eddy momentum flux directly accelerates the jet.

The wavelike response downstream of the SST anomaly has been seen in earlier observational and modeling studies on the atmospheric response to extratropical SST anomalies (e.g., Peng and Whitaker 1999; Liu et al. 2007; Wen et al. 2010; Taguchi et al. 2012). It has been shown that perturbations to the extratropical atmospheric circulation over the North Pacific and the North Atlantic can both generate stationary Rossby wave trains (Palmer and Sun 1985; Honda et al. 2001, 2005) that propagate along the westerly jet acting as a waveguide (Hoskins and Ambrizzi 1993; Branstator 2002) and thus have remote influences over the downstream oceans and continents. Indeed, the North Atlantic atmospheric response to North Pacific SST anomalies has been attributed to the propagation of accumulated stationary Rossby wave activity (Wen et al. 2010; Liu et al. 2012a,b), and the Rossby waveguide effects are found to be responsible for circumglobal teleconnections (Branstator 2002). The wavelike response found here is therefore referred to as a circumglobal Rossby wave train that emanates from the ENP as a result of the eddy-mediated response mechanism.

In quasigeostrophic theory, possible sources of Rossby waves (i.e., perturbations to the mean flow that trigger Rossby waves) include divergence (convergence) of eddy vorticity flux and upper-level divergence (convergence) of the mean flow multiplied by the Coriolis parameter, both driving high (low) pressure at a certain distance downstream of the wave source due to vorticity advection (Hoskins et al. 1983; Sardeshmukh and Hoskins 1988). Over the ENP, the eddy vorticity flux convergence discussed above (Figs. 4a and 5a) appears to be the primary source for changing the mean-flow vorticity and generating Rossby waves, since there the upper-level mean-flow divergence term essentially counteracts the low pressure response (Figs. 3h and 4b). The relatively strong upper-level mean-flow divergence over the ENP is thus the result rather than cause of the low pressure response

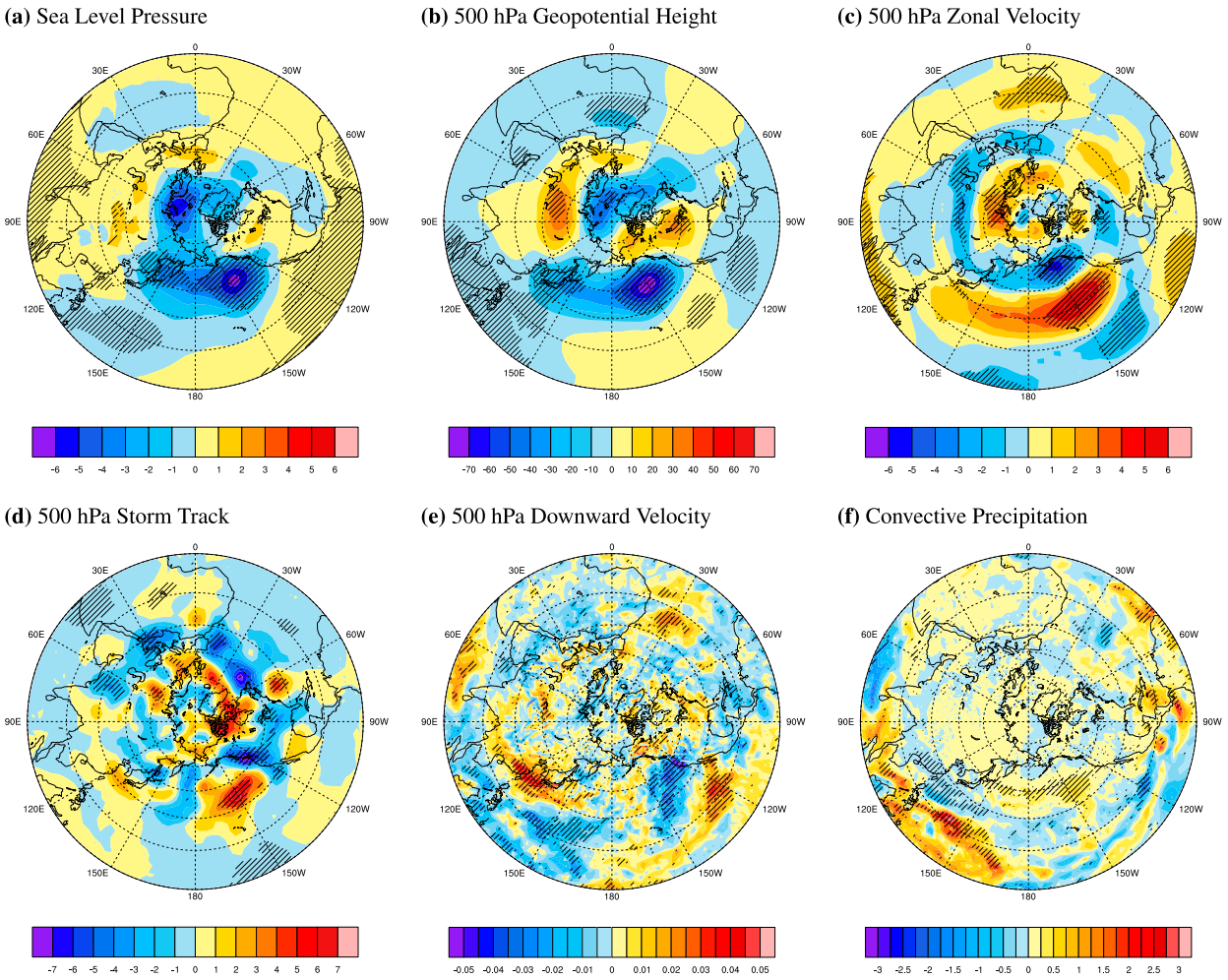

FIG. 3. The 1981–90 decadal-mean winter (DJF) responses of (a) sea level pressure (hPa), (b) 500-hPa geopotential height (m), (c) 500-hPa zonal wind velocity (m s^{-1}), (d) 500-hPa storm track (m) defined as the standard deviation of 2–8-day filtered geopotential height, (e) 500-hPa downward velocity (Pa s^{-1}), and (f) convective precipitation (mm day^{-1}). Statistical significance at the 90% level is indicated by hatching.

driven by the eddy vorticity forcing, and it in turn drives a secondary meridional circulation in the vertical plane resulting in an upper-level convergence upstream and an enhancement of the westerly jet at mid- to lower levels (Fig. 5b). Moreover, the strongest pressure (Figs. 3a,b) and vorticity (not shown) changes appear at the beginning of the wave train instead of at a noticeable distance downstream of the Rossby wave source, which may be attributed to the relatively slow climatological zonal flow over the ENP (Fig. 6a).

Over the WNP, where the storm-track response is weak and insignificant, the mechanism must be different. Although it may sound plausible that the low pressure response over Japan is just the third trough of the eastward-propagating wave train forced in the ENP region, the significant changes in vertical velocity and convective precipitation over the East China Sea and south of it (Figs. 3e,f) suggests another Rossby wave source: the upper-level convergence associated with the secondary circulation over southeast China and the East China Sea driving a positive vorticity anomaly over Japan. Advection by the well-developed jet stream in this region (Fig. 6a) moves the vorticity and pressure response downstream of the wave source (Sardeshmukh and Hoskins 1988).

c. *Decadal-mean response: 1991–2000*

The decadal-mean winter atmospheric response to the PDO-like SST anomaly (Fig. 1) during Dec9100 is remarkably different and considerably weaker in amplitude in the centers of action in comparison to that in Dec8190 (Figs. 3g,h). Particularly, the ENP low pressure response is very weak and statistically insignificant, and the corresponding zonal velocity exhibits little change in that region (Fig. 3i). The

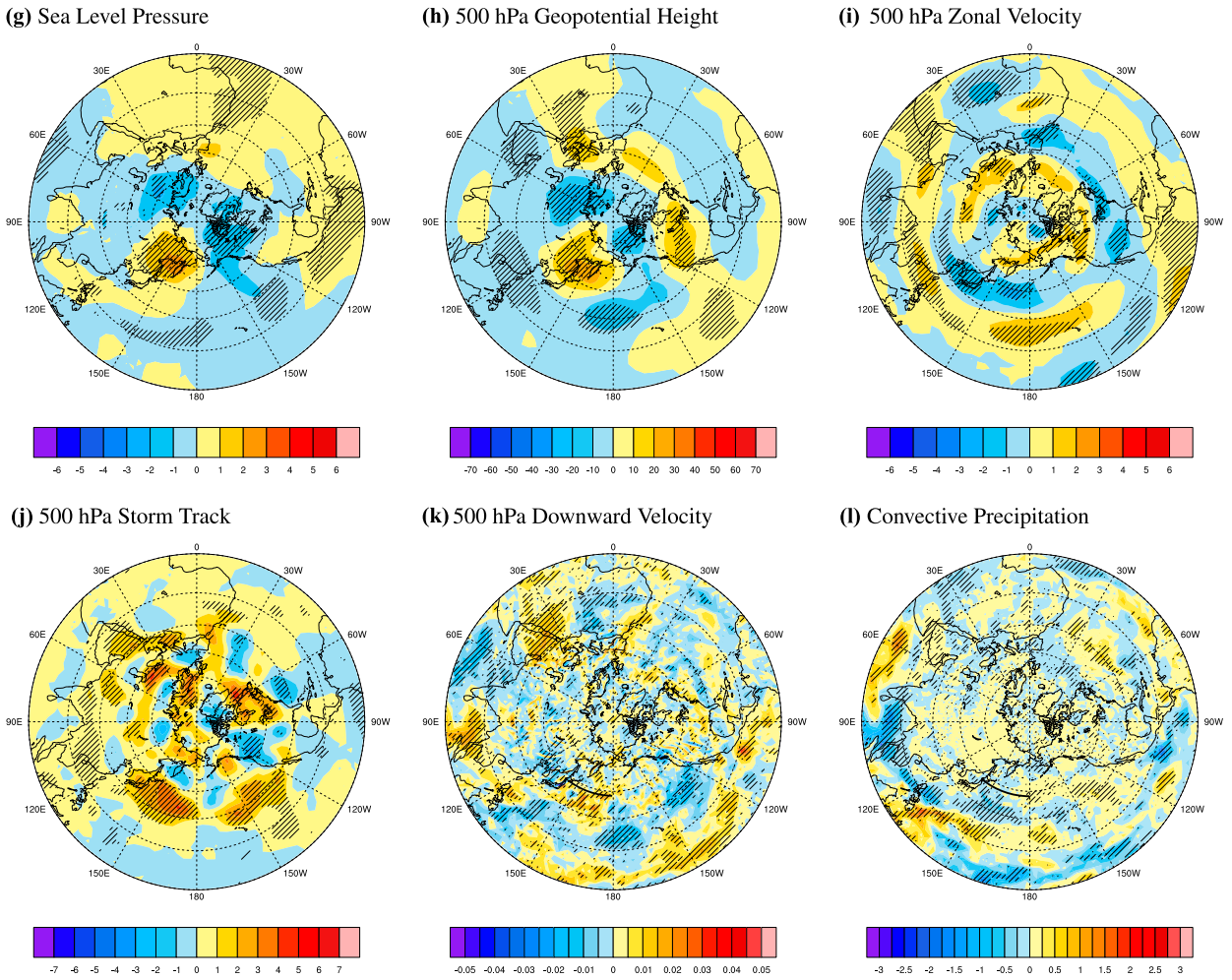

FIG. 3. (continued). The 1991–2000 decadal-mean winter (DJF) responses of (g) sea level pressure (hPa), (h) 500-hPa geopotential height (m), (i) 500-hPa zonal wind velocity ($m\,s^{-1}$), (j) 500-hPa storm track (m) defined as the standard deviation of 2–8-day filtered geopotential height, (k) 500-hPa downward velocity ($Pa\,s^{-1}$), and (l) convective precipitation ($mm\,day^{-1}$). Statistical significance at the 90% level is indicated by hatching. In (k) and (l), the mean position of the Oyashio Extension front is indicated by the black arc.

storm-track response over the ENP becomes much weaker (Fig. 3j) and is associated with reduced vertical velocity and convective precipitation anomalies (Figs. 3k,l). Hence the ENP response in Dec9100 generally exhibits a similar pattern but much reduced amplitude in comparison to that during Dec8190.

More interestingly, the WNP low pressure anomaly is replaced by an equivalent barotropic high pressure anomaly, which also marks the beginning of a wave train (Figs. 3g,h). Correspondingly, the jet stream is locally weakened over the WNP (Fig. 3i). Further, a significant increase of the storm-track response is observed over the WNP (Fig. 3j). The vertical velocity and convective precipitation (Figs. 3k,l) both show a region of significantly reduced convection response on the south flank of the Oyashio Extension front (OEF; Frankignoul et al. 2011; Smirnov et al. 2015; see Fig. 7c). Upstream, a region with upward motion over northeast China and Korea to the Sea of Japan/East Sea (30°–45°N, 110°–150°E) is observed.

In a more global view, the Dec9100 response also takes the form of a stationary Rossby wave train, yet in contrast to the dominating eddy-mediated Rossby wave source in Dec8190, the primary wave source for the Dec9100 response over the WNP is not established by eddy forcing. In particular, the increased storm-track response induces only little eddy vorticity flux convergence over the WNP (Figs. 4c and 5c). In looking for the potential Rossby wave source, one should keep in mind that the WNP is characterized by strong mean westerly winds (Fig. 6b) driving noticeable downstream vorticity advection and that Rossby waves can

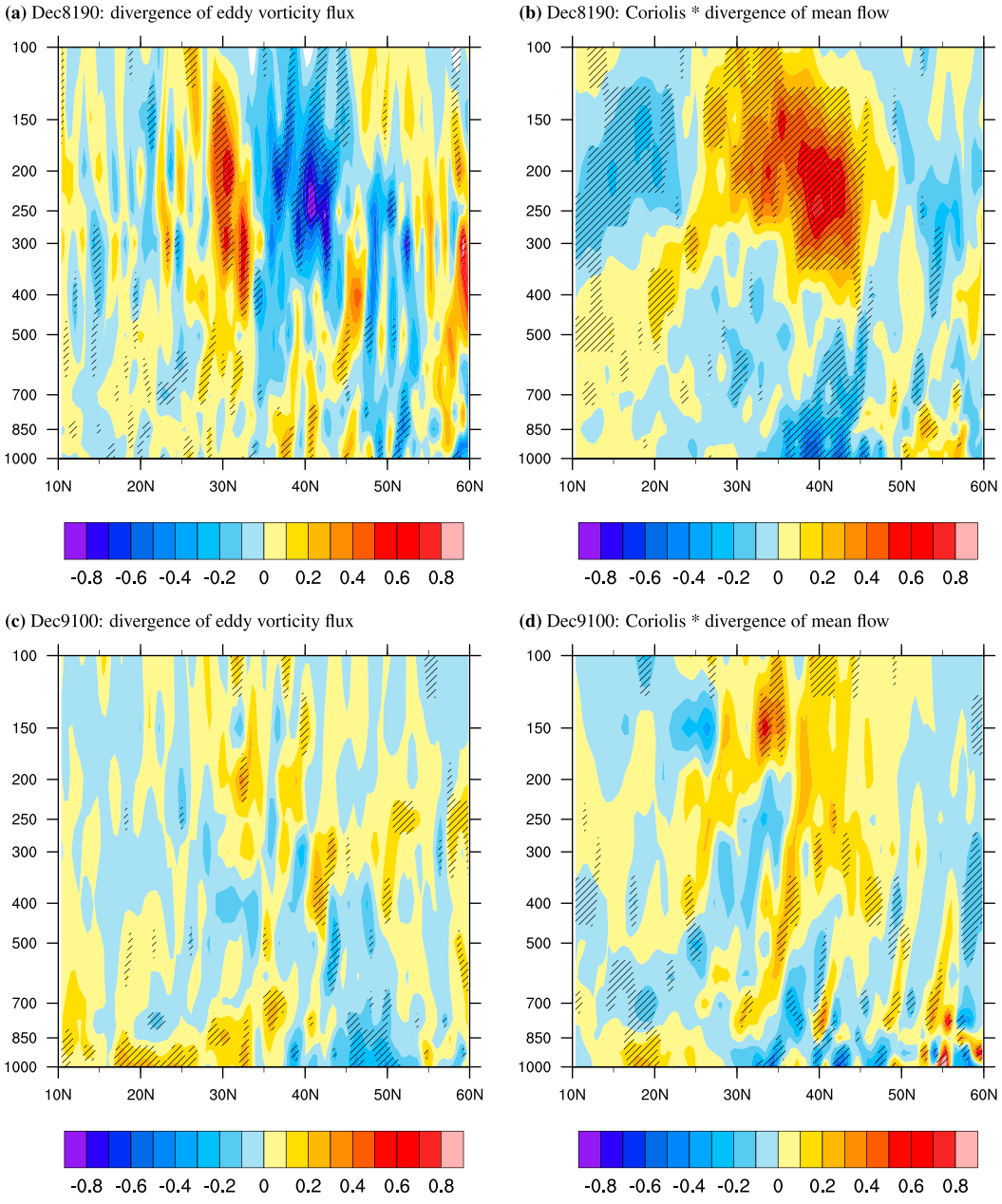

FIG. 4. Zonally averaged decadal-mean winter (DJF) response of the Rossby wave source terms for (a),(b) 1981–90, (c),(d) 1991–2000: (a),(c) divergence of eddy vorticity flux response (day^{-2}) and (b),(d) Coriolis parameter times mean-flow divergence response (day^{-2}). Meridional range: (a),(b) 180°–100°W, (c) 120°–180°E, and (d) 110°–140°E. Statistical significance at the 90% level is indicated by hatching.

propagate poleward. According to the quasigeostrophic vorticity equation (Hoskins et al. 1983) and in the absence of eddy forcing, the high pressure and thus negative vorticity anomalies must be generated by upper-level divergence associated with ascending motion. As a result, the upward vertical velocity response (Fig. 3k) over northeast China to the Sea of Japan/East Sea (30°–45°N, 110°–150°E) associated with strong upper-level divergence (Figs. 4d and 5d) indicates the most likely wave source (Sardeshmukh and Hoskins 1988). The mechanism driving the upward motion is likely to be the compensation of the descending motion south of the OEF (30°–45°N, 150°–180°E; Figs. 3k and 5d).

In summary, a clear decadal regime shift can be inferred from the two experiments: the primary Rossby wave source is due to eddy vorticity flux forcing over the ENP

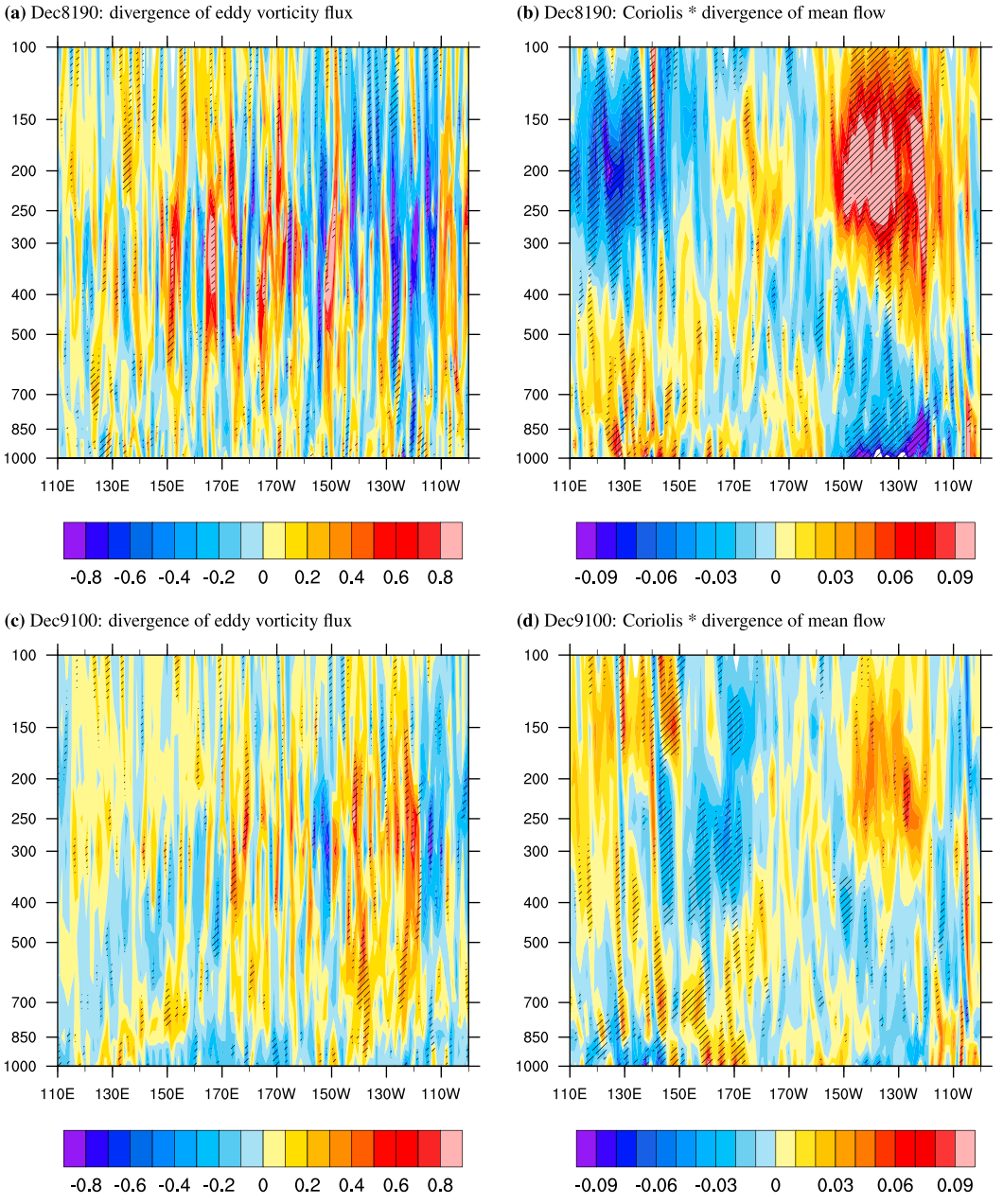

FIG. 5. Meridionally averaged (30°–50°N) decadal-mean winter (DJF) response of the Rossby wave source terms for (a),(b) 1981–90, (c),(d) 1991–2000: (a),(c) divergence of eddy vorticity flux response (day^{-2}) and (b),(d) Coriolis parameter times mean-flow divergence response (day^{-2}). Statistical significance at the 90% level is indicated by hatching.

during Dec8190, while it could perhaps be caused by mean-flow divergence over the WNP during Dec9100.

4. Relation to background circulation changes

Some earlier modeling studies (e.g., Peng et al. 1995; Ting and Peng 1995; Peng et al. 1997; Peng and Whitaker 1999; Taguchi et al. 2012) found that the atmospheric response to extratropical North Pacific SST anomalies exhibits strong dependence on the background atmospheric circulation by comparing the atmospheric response to the same SST anomaly, superimposed on climatological SST for January and February, which forces different atmospheric background states. Although the exact mechanism was not fully explained, they did provide evidence that the

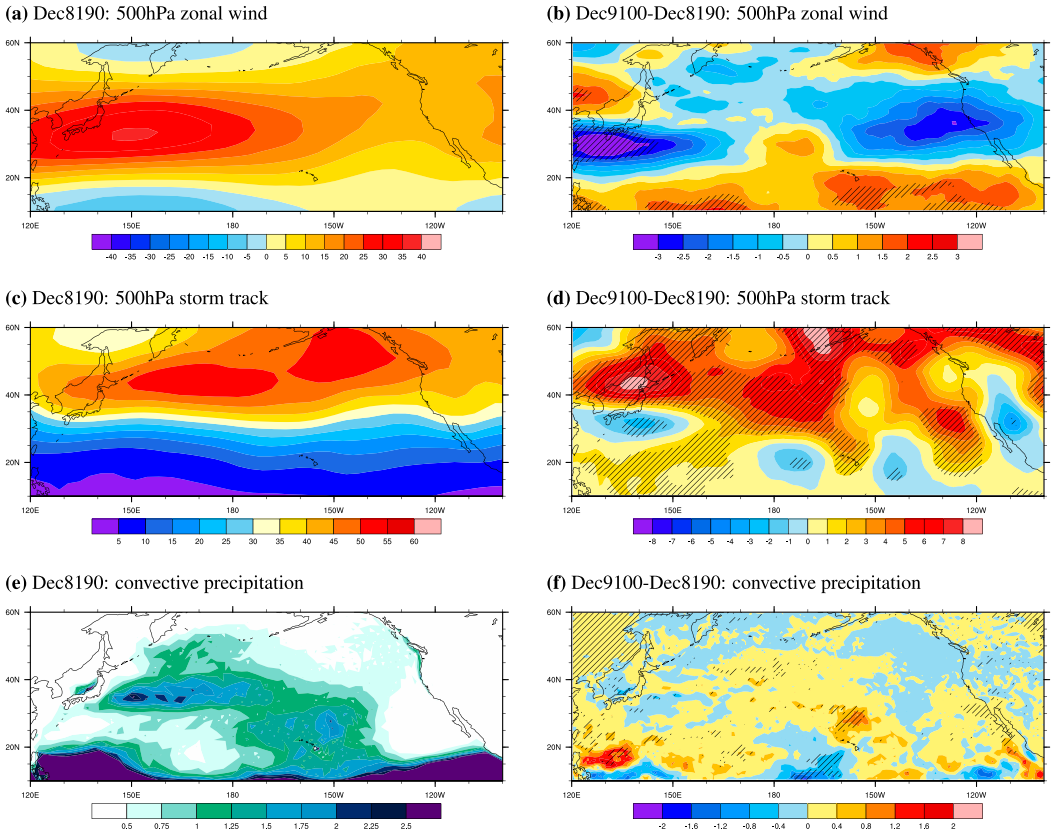

FIG. 6. Decadal-mean atmospheric background state from CTRL for (left) 1981–90 and (right) the difference between 1991–2000 and 1981–90. Statistical significance at the 90% level is indicated by hatching. (a),(b) The 500-hPa zonal wind velocity (m s^{-1}), (c),(d) 500-hPa storm track (m) defined as the standard deviation of 2–8-day filtered geopotential height, and (e),(f) convective precipitation (mm day^{-1}).

influence of the different atmospheric background states is through changing the storm track in the background. We next try to find out the role of the atmospheric background state by analyzing results from our control run.

a. Jet stream

Taking advantage of aquaplanet experiments under perpetual equinox conditions, Brayshaw et al. (2008) proposed an interpretation of the findings of the earlier studies in terms of the position of the anomalous SST gradient relative to that of the background subtropical jet. As shown in Ting and Peng (1995), while the position of the anomalous SST gradient remains the same, the subtropical jet significantly shifts meridionally on seasonal time scales, resulting in different relative position to the SST gradient anomaly in January and February and thus different atmospheric responses according to Brayshaw et al. (2008).

In trying to explain the different decadal response regimes found in this study, we follow Brayshaw et al. (2008) and compare the position of the background subtropical jet in the two decades simulated by CTRL. As depicted in Figs. 6a,b, there is only one jet stream over the North Pacific in both decades, being a merge of the subtropical jet and the eddy-driven polar-front jet in winter (Lee and Kim 2003). However, except at the jet entrance, the position of the North Pacific jet does not exhibit perceptible changes over the two decades, indicating much less meridional variation of the winter jet on decadal time scales than on seasonal time scales. As a result, in the sense of decadal mean, the difference of the atmospheric response cannot be attributed to the shift of the subtropical jet in the background circulation.

b. Storm track

The midlatitude storm track is shown to undergo significant intensification during recent decades, as revealed by statistical assessment on reanalysis products (Gan and Wu 2012) and consistent with twenty-first-century climate projections from the IPCC AR4 (Yin 2005). In our CTRL experiment, the

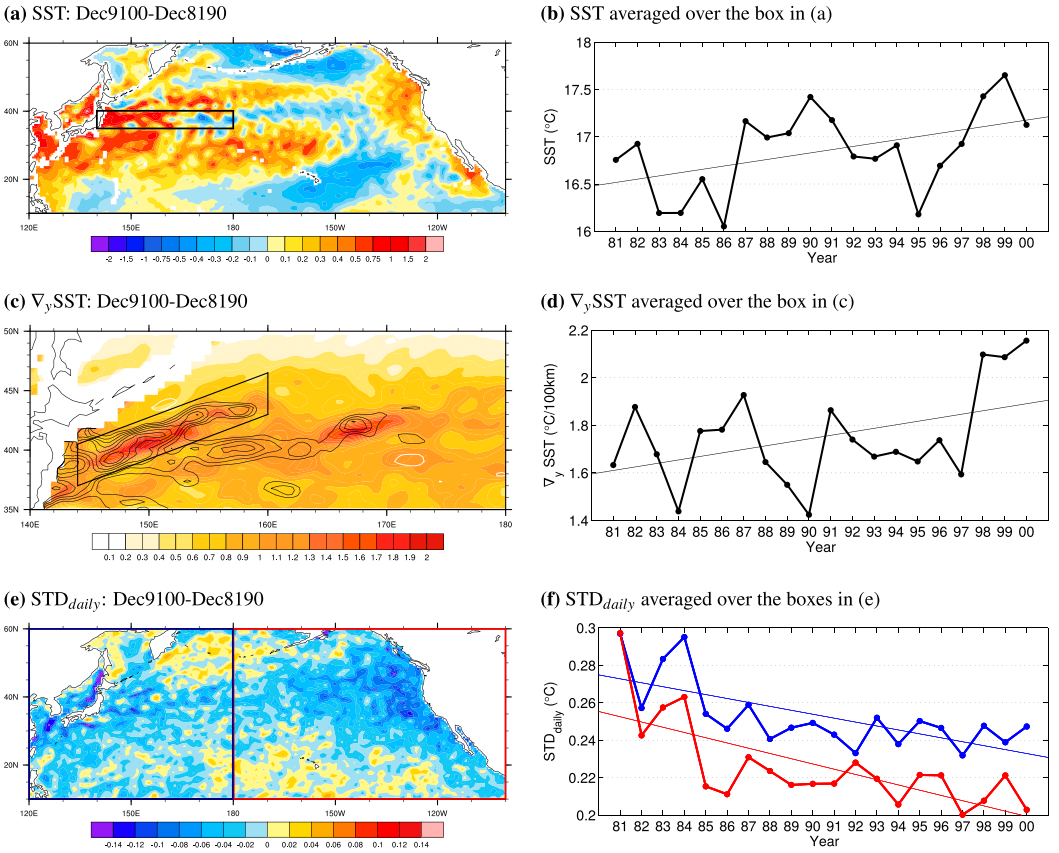

FIG. 7. (left) Difference (Dec9100 minus Dec8190) of decadal-mean (a) SST (°C) (contours) meridional SST gradient [°C (100 km)$^{-1}$] Black and blue contours respectively stand for positive and negative values. Contours start at ±0.4 with interval 0.2. Shading shows Dec8190 mean. (e) Standard deviation of daily SST variability (°C). (right) Time series averaged over the boxes indicated in (left). Solid lines show the linear trends. All trends pass the *t* test at the 95% level.

decadal-mean storm track simulated for Dec8190 and Dec9100 shows general agreement with this finding (Figs. 6c,d). Such intensification, as pointed out by Gan and Wu (2012), would presumably amplify the midlatitude transient eddy feedback and thus the eddy-mediated atmospheric response to extratropical SST anomalies. However, as shown above, in our modeling results the eddy-mediated response over the ENP is dramatically reduced in Dec9100 compared to Dec8190 and is replaced by the divergence-driven response over the WNP, even though Dec9100 is warmer than Dec8190 (Figs. 7a,b). As mysterious as it is, this means the difference of the decadal-mean atmospheric response cannot be traced back to differences of the background storm track according to current understanding.

c. *Deep convection associated with sharp SST fronts*

Considering the divergence-driven response in Dec9100 associated with changes of vertical convection, we first notice a climatological deep convection zone south of the OEF, as indicated by the convective rainfall derived from CTRL (Figs. 6e,f). In the North Atlantic south of the Gulf Stream front, Minobe et al. (2008) found such a deep convection zone and associated heavy rainfall, high clouds, and upper-level divergence. Regarding the mechanism, they proposed that the deep convection zone is maintained by the SST front through pressure adjustment. Taguchi et al. (2009) presented similar findings for the North Pacific in the Kuroshio/Oyashio Extension region.

As discussed above, the Dec9100 response is characterized by a convection anomaly in the location of the deep convection zone. It is thus natural to speculate about the decadal difference of the deep convection zone in the background state being the reason for the different response in the two decades. However, Figs. 6e,f do not show a clear contrast in the deep convection zone in CTRL, effectively negating such speculation. It is nevertheless conceivable that the

deep convection response in Dec9100 is forced by perturbations to the OEF induced by the SST anomaly.

To summarize, the results obtained from the control integration (without superimposing an SST anomaly) do not provide evidence for the atmospheric background changes being responsible for the differences in the response between the two decades.

5. Relation to background SST changes

Previous studies (e.g., Peng et al. 1995; Ting and Peng 1995; Peng et al. 1997; Peng and Whitaker 1999; Taguchi et al. 2012) used different climatological background SST to force the model and found a different atmospheric response to the same SST anomaly, yet they focused only on investigating the role of the atmospheric background circulation, without touching the potential importance of the background SST. Having tried to find the role of the background atmospheric circulation in the last section, here, as in Z15, we try to link the atmospheric response to the change in the background SST. Z15 have highlighted the essential role of the daily variability of the background SST. Here we take the view that the decadal regime shift in the response discussed above in section 3 must be related to decadal changes of background SST since the background SST is the only thing changing over the decades in our experimental setup.

a. Decadal SST changes in the North Pacific

During 1981–2000, the North Pacific SST experienced substantial decadal changes. Figures 7a,b depict that the SST is characterized by significant warming in many regions of the North Pacific, especially over the WNP (see also Wu et al. 2012). On the other hand, important spatial features and high-frequency SST variability have undergone remarkable decadal change as well. Frankignoul et al. (2011) and Smirnov et al. (2015) presented monthly OEF indices derived from observations, which, in the sense of decadal mean, would suggest a northward shift of the OEF in Dec9100 compared to Dec8190. As shown in Smirnov et al. (2015), with such a shift, only the northern edge of the region of high meridional gradient penetrates northward, while the southern edge remains in the same location, and the maximum gradient is essentially unchanged. This would result in greater SST difference over the latitudinal range of high SST gradient in the second decade. Our results of the difference of decadal-mean SST gradient (Figs. 7c,d) also indicate that the OEF is stronger in Dec9100 compared to Dec8190, with less evident a shift. Moreover, the level of high-frequency (i.e., daily) SST variability dropped dramatically over both the western and eastern parts of the basin, with the region off the west coast of North America being one of the most noticeable regions (Figs. 7e,f). These decadal changes modify the background SST on which the SST anomaly is applied. However, though interesting, understanding the dynamics behind the decadal SST changes is beyond the scope of this paper.

b. The emergence of the WNP divergence-driven wave source

The boundary between the positive and negative SST anomalies (Fig. 1) is roughly aligned with the OEF. The positive polarity of the SST anomaly forcing, as well as the difference (positive minus negative) between the polarities, thus reduces the strength of the front. This perturbation to the frontal strength, by definition, acts in both decades, yet with rather different effects. In Dec8190, no significant response in vertical velocity and convective precipitation is simulated over the deep convection zone. The anomalies in the two variables rather closely follow the SST anomaly pattern in the East China Sea and east of the Philippines (Figs. 3e,f), suggesting a direct connection. In Dec9100, on the other hand, the response in vertical velocity and convective precipitation shows little pattern correlation with the SST anomaly in this region (Figs. 3k,l), rather primarily taking place over the deep convection zone associated with the OEF. We hypothesize that the atmosphere is more sensitive to OEF perturbations in the context of a stronger OEF. In particular, when the OEF is relatively weak, as in Dec8190, OEF perturbations are not very effective in driving a significant atmospheric response.

c. The degeneration of the ENP eddy-driven wave source

Z15 recently showed by analyzing modeling results that retaining daily variability in the background SST plays a key role in the eddy-driven atmospheric response, especially over the ENP. In particular, they found anomalously strong storm-track response when daily variability is included in the North Pacific background SST, which is associated with anomalous baroclinicity and surface heat transfer. We return to this type of response below. Here the primary Rossby wave source in Dec8190 is the eddy vorticity divergence over the ENP (Figs. 3a,b), which, as argued by Z15, is sensitive to daily background SST variability. The decadal downward trend in the level of daily SST variability (Figs. 7e,f) is then presumably indicative of a reduction

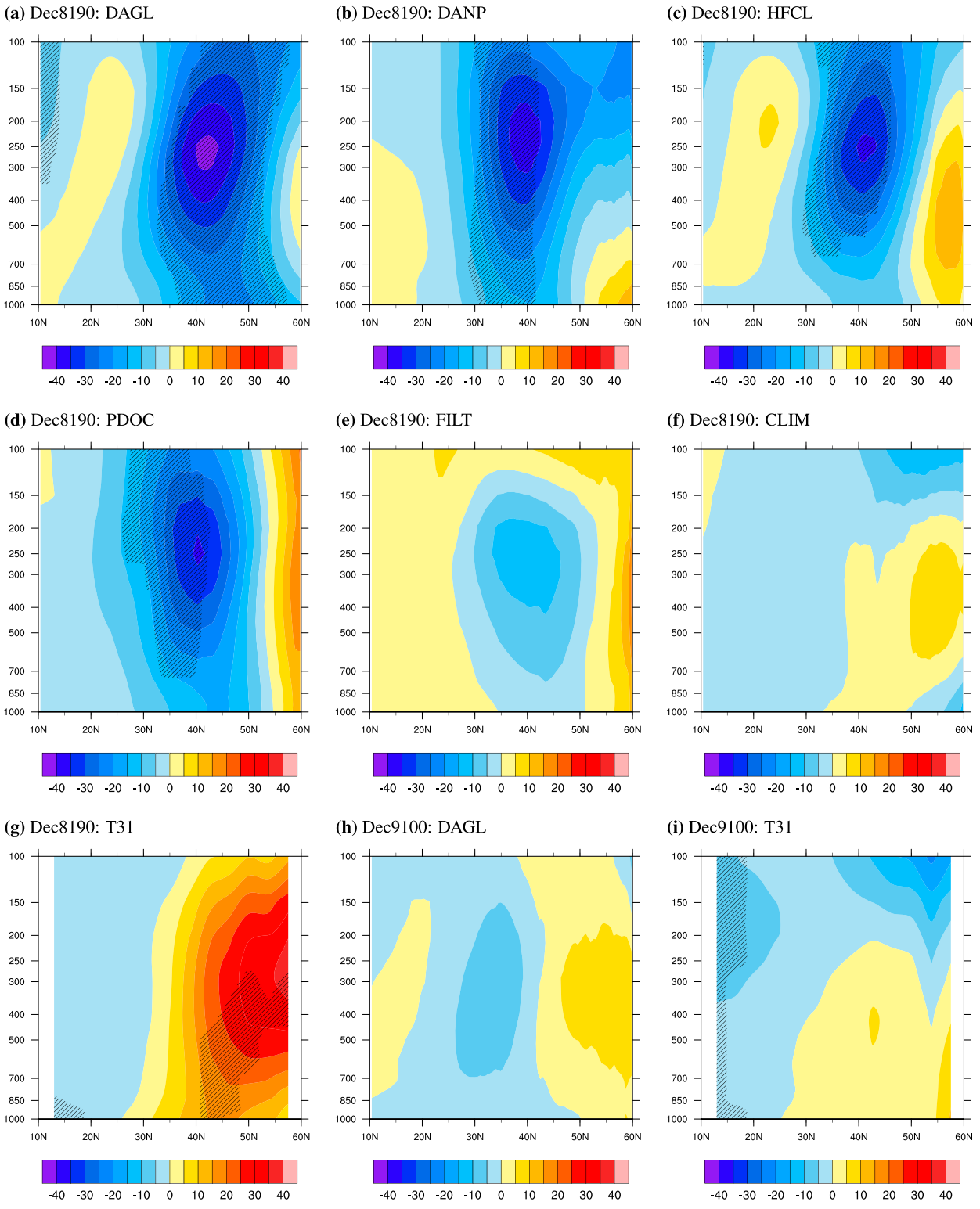

FIG. 8. Vertical sections of (a)–(g) 1981–90 and (h),(i) 1991–2000 decadal-mean winter (DJF) response zonally averaged over the North Pacific sector (10°–60°N, 120°E–100°W) for geopotential height (m) simulated in various experiments (described in Table 1): (a),(h) DAGL, (b) DANP, (c) HFCL, (d) PDOC, (e) FILT, (f) CLIM, and (g),(i) the T31 experiment. (b) DAGL, (c) HFCL, (e) FILT, and (f) CLIM are presented by Z15; (a)–(d) preserve daily background SST, and (e),(f),(g) have reduced daily background SST. The T31 experiment allows for daily background SST but with coarse spatial resolution. Statistical significance at the 90% level is indicated by hatching.

TABLE 1. List of experiments. All SST anomalies are only applied to the North Pacific. See section 2 for data source and SST anomaly generation. For resolution, T*X*L*Y* means T*X* horizontal grid and L*Y* vertical levels.

Period	Name	SST anomaly	Background SST		Resolution
			North Pacific	Other oceans	
Dec8190	CTRL	None	Daily observed	Daily observed	T213L31
	DAGL	PDO-like	Daily observed	Daily observed	T213L31
	DANP	PDO-like	Daily observed	Decadal climatology	T213L31
	HFCL	PDO-like	High-pass (11 day) filtered	Decadal climatology	T213L31
	PDOC	PDO cold	Daily observed	Daily observed	T213L31
	FILT	PDO-like	Low-pass (11 day) filtered	Decadal climatology	T213L31
	CLIM	PDO-like	Decadal climatology	Decadal climatology	T213L31
	T31	PDO-like	Daily observed	Daily observed	T31L19
Dec9100	CTRL	None	Daily observed	Daily observed	T213L31
	DAGL	PDO-like	Daily observed	Daily observed	T213L31
	T31	PDO-like	Daily observed	Daily observed	T31L19

of the eddy-driven wave source, thus providing a possible explanation for the difference of the ENP response to identical SST anomalies during the two decades.

In summary, in our experiments, we found that the relative importance of the Rossby wave sources in the WNP and ENP can eventually determine the atmospheric response to identical extratropical SST anomalies, and the Rossby wave sources themselves can be driven by respective components of the background SST such as daily variability and the OEF.

6. Summary and discussion

Using a global high-resolution atmospheric general circulation model (AGCM), we have investigated the wintertime (DJF) atmospheric response to identical extratropical North Pacific sea surface temperature (SST) anomalies superimposed on daily varying background SST for the two adjacent decades 1981–2000. The decadal-mean responses in the two decades vastly differ both in terms of sign and amplitude, yet they can both be characterized by a Rossby wave train. However, the primary mechanism and location of the wave source are rather different. In the first decade, the response is dominated by eddy vorticity flux forcing over the eastern North Pacific (ENP) together with a secondary wave source over the western North Pacific (WNP) directly related to the SST anomaly. In the second decade, mean-flow divergence over the WNP presumably becomes the primary wave source, whereas the eddy-driven wave source over the ENP substantially decays. The model results can be understood as a regime shift in the response between the two decades, with significant changes in the character of the decadal-mean geopotential height response.

The possibility of a regime shift of the response on decadal or even longer time scales is supported by Gan and Wu (2012). We hypothesize that the origin of the regime shift in the response can be traced back to decadal background SST changes. These comprise decadal changes in mean SST, level of daily SST variability, and strength of the Oyashio Extension front (OEF).

To further disentangle the roles of the different components of both the background SSTs and the SST anomaly forcing in driving the atmospheric response a number of sensitivity experiments (see also Z15) were conducted. These comprise experiments with truncated SST anomaly forcing, different model resolution, and different background SSTs on which the SST anomaly forcing was superimposed. Figure 8 and Table 1 summarize all experiments which have been performed for the two decades. As pointed out in Z15, the response during the first decade strongly depends on sufficient daily SST variability over the eastern North Pacific (Figs. 8a–d; experiments DAGL, DANP, HFCL, FILT, and CLIM). During the second decade, the reduced daily SST variability tends to damp the eddy-mediated response (Fig. 8h; experiment DAGL), which in conjunction with the strengthening of the OEF makes the atmosphere more sensitive to SST anomalies in the OEF region, producing a more significant response in the deep convection zone south of the OEF that overrides the secondary wave source noted in the previous decade.

There are small SST anomalies in the SST forcing pattern south of 20°N, especially in the western and far-eastern tropical Pacific (Fig. 1). Since the atmosphere is more sensitive to SST at low latitudes, these anomalies, albeit small but located in the zone of substantial deep convection, may play a role in the extratropical

response. We repeated the DAGL experiment for the 1981–90 decade by retaining only the major cold SST anomaly in the North Pacific seen in Fig. 1. This pattern is referred to as the ''PDO cold'' SST anomaly. We force the model with both the positive and negative polarity of this pattern. Most of the tropical SST anomalies south of 20°N are thus removed. It can be inferred that the atmospheric response to the PDO cold SST anomaly (Fig. 8d; experiment PDOC) resembles that to the PDO-like anomaly (Fig. 8a; experiment DAGL). We conclude that the small tropical SST anomalies are not important to the extratropical atmospheric response.

Moreover, we show that high atmospheric resolution should be employed when studying the atmospheric response to extratropical SST anomalies. For example, when repeating the experiment DAGL with a coarse horizontal resolution (T31, ~3.75°) version, the model simulates a significant but opposite response in 1981–90 and no significant response in 1991–2000 (Figs. 8g,i; experiments T31). This emphasizes the need for sufficiently high horizontal model resolution to resolve eddy dynamics and frontal zone processes.

We have used prescribed SSTs in the atmosphere model experiments presented in this study. While this approach enables designing experiments to isolate the effects of the various components of both the background SSTs and the SST anomaly forcing, the methodology is still under debate. Barsugli and Battisti (1998), for example, showed by a linear stochastic model that in experiments with prescribed SSTs, the heat flux at low frequencies is likely to be too large and of the wrong sign. However, their conclusions do not necessarily apply here because 1) as pointed out by Z15, the PDO-like SST anomaly can be generated by oceanic processes (e.g., the reemergence mechanism; see also Alexander et al. 1999; Czaja and Frankignoul 1999, 2002), whereas in the Barsugli and Battisti (1998) theoretical model the SST anomaly is generated purely by atmospheric variability; and 2) Barsugli and Battisti (1998) showed that the inconsistencies introduced by prescribed SSTs becomes most apparent on time scales longer than seasonal, while we investigate the winter-mean atmospheric response. An argument on the limitations of prescribed SSTs that may apply here was made by Liu and Wu (2004), who performed 2-month simulations using both forced atmosphere model and coupled ocean–atmosphere model simulations to study the influences of coupling on the atmospheric response to a possibly ocean-generated SST anomaly in the North Pacific. Their findings suggest that with prescribed SSTs, although the heat flux is indeed too large, the atmospheric response to the prescribed SST anomaly is of the correct sign but 2 times weaker than in the coupled experiment. They also argued that on monthly time scales, using prescribed SSTs can be a reasonable approximation to reality because the method assumes an infinite heat capacity of the ocean, which is a good approximation in winter when the mixed layer is rather deep. Based on the above discussion, we believe that uncoupled atmosphere model experiments with prescribed SSTs are useful to obtain insight into the mechanisms involved in the atmospheric response to extratropical SST variability.

Our AGCM results shed some light on the long-standing problem of the state dependence of the atmospheric response to extratropical SST anomalies. While previous investigations primarily studied the seasonality of the atmospheric response, we investigated decadal changes of the response. Furthermore, we connect the decadal changes in atmospheric response to decadal changes in the background SST. Our results are of particular importance to the fields of large-scale atmosphere–ocean interactions and climate modeling, as well as decadal climate variability and predictability. Both eddy and frontal processes are suggested to be important in understanding decadal variability of the atmospheric response to extratropical SST anomalies.

Acknowledgments. Guidi Zhou was financially supported by the Chinese Scholarship Council (CSC; 2011633094). This work has been supported by the Cluster of Excellence ''The Future Ocean'' of the German Research Foundation (DFG), the German Ministry for Education and Research (BMBF) through MiKlip2, subproject 01LP1517D (ATMOS-MODINI), RACE (03F0651B), and the EU Project NACLIM (308299). Traveling and other support from GEOMAR is acknowledged. NOAA Extended Reconstructed SST and SLP data are provided by the NOAA/OAR/ESRL/PSD, Boulder, Colorado. Computing resources at the North-German Supercomputing Alliance (HLRN) are acknowledged. We are also grateful to comments from two anonymous reviewers that were helpful for improving the manuscript.

APPENDIX

Significance Tests

a. Decadal means

To test the statistical significance of the decadal-mean winter atmospheric response [i.e., the winter-mean

difference between the positive (P) and negative (N) SST anomaly cases], we use a one-sample t test with 9 degrees of freedom for Dec8190 and 19 for Dec9100. This approach is appropriate because of the following considerations:

1) We test the mean of the difference between the P and N integrations rather than their equality using a two-sample test because the P and N integrations for a certain winter are started from the same initial condition and thus potentially correlated.
2) In our experimental setup, the background SST forcing varies from winter to winter; thus the 10 winters do not strictly form an ensemble. This is roughly overcome by taking the difference between the P and N integrations with the same background SST.
3) Each winter, simulations are started from initial conditions taken one year apart from the control run and are considered independent assuming that the atmospheric states are decorrelated.
4) The integrations for each winter during 1991–2000 are started from 1 November and 1 December conditions from the control run. These two integrations are considered roughly independent after confirming that their multiyear correlation is generally smaller than 0.2 in the hatched regions of Fig. 3h.

b. *Linear trends*

The linear trends of the multiyear time series of the winter-mean atmospheric response are estimated using the least squares estimator and are tested with a one-sample t test using 18 degrees of freedom.

REFERENCES

Alexander, M. A., C. Deser, and M. S. Timlin, 1999: The reemergence of SST anomalies in the North Pacific Ocean. *J. Climate*, **12**, 2419–2433, doi:10.1175/1520-0442(1999)012<2419:TROSAI>2.0.CO;2.

Barsugli, J. J., and D. S. Battisti, 1998: The basic effects of atmosphere–ocean thermal coupling on midlatitude variability. *J. Atmos. Sci.*, **55**, 477–493, doi:10.1175/1520-0469(1998)055<0477:TBEOAO>2.0.CO;2.

Bjerknes, J., 1964: Atlantic air-sea interaction. *Advances in Geophysics*, Vol. 10, Academic Press, 1–82.

Branstator, G., 2002: Circumglobal teleconnections, the jet stream waveguide, and the North Atlantic Oscillation. *J. Climate*, **15**, 1893–1910, doi:10.1175/1520-0442(2002)015<1893:CTTJSW>2.0.CO;2.

Brayshaw, D. J., B. J. Hoskins, and M. Blackburn, 2008: The storm-track response to idealized SST perturbations in an aquaplanet GCM. *J. Atmos. Sci.*, **65**, 2842–2860, doi:10.1175/2008JAS2657.1.

Cayan, D. R., 1992a: Latent and sensible heat-flux anomalies over the northern oceans: The connection to monthly atmospheric circulation. *J. Climate*, **5**, 354–369, doi:10.1175/1520-0442(1992)005<0354:LASHFA>2.0.CO;2.

——, 1992b: Latent and sensible heat flux anomalies over the northern oceans: Driving the sea surface temperature. *J. Phys. Oceanogr.*, **22**, 859–881, doi:10.1175/1520-0485(1992)022<0859:LASHFA>2.0.CO;2.

——, 1992c: Variability of latent and sensible heat fluxes estimated using bulk formulas. *Atmos.–Ocean*, **30**, 1–42, doi:10.1080/07055900.1992.9649429.

Chang, E. K. M., S. Lee, and K. L. Swanson, 2002: Storm track dynamics. *J. Climate*, **15**, 2163–2183, doi:10.1175/1520-0442(2002)015<02163:STD>2.0.CO;2.

Czaja, A., and C. Frankignoul, 1999: Influence of the North Atlantic SST on the atmospheric circulation. *Geophys. Res. Lett.*, **26**, 2969–2972, doi:10.1029/1999GL900613.

——, and ——, 2002: Observed impact of Atlantic SST anomalies on the North Atlantic Oscillation. *J. Climate*, **15**, 606–623, doi:10.1175/1520-0442(2002)015<0606:OIOASA>2.0.CO;2.

Deser, C., and M. L. Blackmon, 1993: Surface climate variations over the North Atlantic Ocean during winter: 1900–1989. *J. Climate*, **6**, 1743–1753, doi:10.1175/1520-0442(1993)006<1743:SCVOTN>2.0.CO;2.

Frankignoul, C., 1985: Sea surface temperature anomalies, planetary waves, and air-sea feedback in the middle latitudes. *Rev. Geophys.*, **23**, 357–390, doi:10.1029/RG023i004p00357.

——, and N. Sennéchael, 2007: Observed influence of North Pacific SST anomalies on the atmospheric circulation. *J. Climate*, **20**, 592–606, doi:10.1175/JCLI4021.1.

——, ——, Y. O. Kwon, and M. A. Alexander, 2011: Influence of the meridional shifts of the Kuroshio and the Oyashio Extensions on the atmospheric circulation. *J. Climate*, **24**, 762–777, doi:10.1175/2010JCLI3731.1.

Gan, B., and L. Wu, 2012: Modulation of atmospheric response to North Pacific SST anomalies under global warming: A statistical assessment. *J. Climate*, **25**, 6554–6566, doi:10.1175/JCLI-D-11-00493.1.

Gates, W. L., and Coauthors, 1999: An overview of the results of the Atmospheric Model Intercomparison Project (AMIP I). *Bull. Amer. Meteor. Soc.*, **80**, 29–55, doi:10.1175/1520-0477(1999)080<0029:AOOTRO>2.0.CO;2.

Gulev, S. K., M. Latif, N. S. Keenlyside, W. Park, and K. P. Koltermann, 2013: North Atlantic Ocean control on surface heat flux on multidecadal timescales. *Nature*, **499**, 464–467, doi:10.1038/nature12268.

Honda, M., H. Nakamura, J. Ukita, I. Kousaka, and K. Takeuchi, 2001: Interannual seesaw between the Aleutian and Icelandic lows. Part I: Seasonal dependence and life cycle. *J. Climate*, **14**, 1029–1042, doi:10.1175/1520-0442(2001)014<1029:ISBTAA>2.0.CO;2.

——, Y. Kushnir, H. Nakamura, S. Yamane, and S. E. Zebiak, 2005: Formation, mechanisms, and predictability of the Aleutian–Icelandic low seesaw in ensemble AGCM simulations. *J. Climate*, **18**, 1423–1434, doi:10.1175/JCLI3353.1.

Hoskins, B. J., and T. Ambrizzi, 1993: Rossby wave propagation on a realistic longitudinally varying flow. *J. Atmos. Sci.*, **50**, 1661–1671, doi:10.1175/1520-0469(1993)050<1661:RWPOAR>2.0.CO;2.

——, I. N. James, and G. H. White, 1983: The shape, propagation and mean-flow interaction of large-scale weather systems. *J. Atmos. Sci.*, **40**, 1595–1612, doi:10.1175/1520-0469(1983)040<1595:TSPAMF>2.0.CO;2.

Kushnir, Y., 1994: Interdecadal variations in North Atlantic sea surface temperature and associated atmospheric conditions. *J. Climate*, **7**, 141–157, doi:10.1175/1520-0442(1994)007<0141:IVINAS>2.0.CO;2.

——, and I. M. Held, 1996: Equilibrium atmospheric response to North Atlantic SST anomalies. *J. Climate*, **9**, 1208–1220, doi:10.1175/1520-0442(1996)009<1208:EARTNA>2.0.CO;2.

——, W. A. Robinson, I. Bladé, N. M. J. Hall, S. Peng, and R. Sutton, 2002: Atmospheric GCM response to extratropical SST anomalies: Synthesis and evaluation. *J. Climate*, **15**, 2233–2256, doi:10.1175/1520-0442(2002)015<2233:AGRTES>2.0.CO;2.

Kwon, Y.-O., and C. Deser, 2007: North Pacific decadal variability in the Community Climate System Model version 2. *J. Climate*, **20**, 2416–2433, doi:10.1175/JCLI4103.1.

Latif, M., and T. P. Barnett, 1994: Causes of decadal climate variability over the North Pacific and North America. *Science*, **266**, 634–637, doi:10.1126/science.266.5185.634.

——, and ——, 1996: Decadal climate variability over the North Pacific and North America: Dynamics and predictability. *J. Climate*, **9**, 2407–2423, doi:10.1175/1520-0442(1996)009<2407:DCVOTN>2.0.CO;2.

Lee, D. E., Z. Liu, and Y. Liu, 2008: Beyond thermal interaction between ocean and atmosphere: On the extratropical climate variability due to the wind-induced SST. *J. Climate*, **21**, 2001–2018, doi:10.1175/2007JCLI1532.1.

Lee, S., and H. Kim, 2003: The dynamical relationship between subtropical and eddy-driven jets. *J. Atmos. Sci.*, **60**, 1490–1503, doi:10.1175/1520-0469(2003)060<1490:TDRBSA>2.0.CO;2.

Li, Q., 2006: Climatological analysis of planetary wave propagation in Northern Hemisphere winter. Max Planck Institute for Meteorology Earth System Science Rep. 35, 160 pp. [Available online at https://www.mpimet.mpg.de/fileadmin/publikationen/Reports/WEB_BzE_35.pdf.]

Liu, Q., N. Wen, and Z. Liu, 2006: An observational study of the impact of the North Pacific SST on the atmosphere. *Geophys. Res. Lett.*, **33**, L18611, doi:10.1029/2006GL026082.

Liu, Z., and L. Wu, 2004: Atmospheric response to North Pacific SST: The role of ocean–atmosphere coupling. *J. Climate*, **17**, 1859–1882, doi:10.1175/1520-0442(2004)017<1859:ARTNPS>2.0.CO;2.

——, Y. Liu, L. Wu, and R. Jacob, 2007: Seasonal and long-term atmospheric responses to reemerging North Pacific Ocean variability: A combined dynamical and statistical assessment. *J. Climate*, **20**, 955–980, doi:10.1175/JCLI4041.1.

——, L. Fan, S. I. Shin, and Q. Liu, 2012a: Assessing atmospheric response to surface forcing in the observations. Part II: Cross validation of seasonal response using GEFA and LIM. *J. Climate*, **25**, 6817–6834, doi:10.1175/JCLI-D-11-00630.1.

——, N. Wen, and L. Fan, 2012b: Assessing atmospheric response to surface forcing in the observations. Part I: Cross validation of annual response using GEFA, LIM, and FDT. *J. Climate*, **25**, 6796–6816, doi:10.1175/JCLI-D-11-00545.1.

Ma, X., and Coauthors, 2016: Western boundary currents regulated by interaction between ocean eddies and the atmosphere. *Nature*, **535**, 533–537, doi:10.1038/nature18640.

Mantua, N. J., S. R. Hare, Y. Zhang, J. M. Wallace, and R. C. Francis, 1997: A Pacific interdecadal climate oscillation with impacts on salmon production. *Bull. Amer. Meteor. Soc.*, **78**, 1069–1079, doi:10.1175/1520-0477(1997)078<1069:APICOW>2.0.CO;2.

Minobe, S., A. Kuwano-Yoshida, N. Komori, S.-P. Xie, and R. J. Small, 2008: Influence of the Gulf Stream on the troposphere. *Nature*, **452**, 206–209, doi:10.1038/nature06690.

Nakamura, H., G. Lin, and T. Yamagata, 1997: Decadal climate variability in the North Pacific during the recent decades. *Bull. Amer. Meteor. Soc.*, **78**, 2215–2225, doi:10.1175/1520-0477(1997)078<2215:DCVITN>2.0.CO;2.

Neelin, J. D., D. S. Battisti, A. C. Hirst, F.-F. Jin, Y. Wakata, T. Yamagata, and S. E. Zebiak, 1998: ENSO theory. *J. Geophys. Res.*, **103**, 14 261–14 290, doi:10.1029/97JC03424.

Palmer, T. N., and Z. Sun, 1985: A modelling and observational study of the relationship between sea surface temperature in the northwest Atlantic and the atmospheric general circulation. *Quart. J. Roy. Meteor. Soc.*, **111**, 947–975, doi:10.1002/qj.49711147003.

Peng, S., and J. S. Whitaker, 1999: Mechanisms determining the atmospheric response to midlatitude SST anomalies. *J. Climate*, **12**, 1393–1408, doi:10.1175/1520-0442(1999)012<1393:MDTART>2.0.CO;2.

——, L. A. Mysak, J. Derome, H. Ritchie, and B. Dugas, 1995: The difference between early and middle winter atmospheric response to sea surface temperature anomalies in the northwest Atlantic. *J. Climate*, **8**, 137–157, doi:10.1175/1520-0442(1995)008<0137:TDBEAM>2.0.CO;2.

——, W. A. Robinson, and M. P. Hoerling, 1997: The modeled atmospheric response to midlatitude SST anomalies and its dependence on background circulation states. *J. Climate*, **10**, 971–987, doi:10.1175/1520-0442(1997)010<0971:TMARTM>2.0.CO;2.

Reynolds, R. W., T. M. Smith, C. Liu, D. B. Chelton, K. S. Casey, and M. G. Schlax, 2007: Daily high-resolution-blended analyses for sea surface temperature. *J. Climate*, **20**, 5473–5496, doi:10.1175/2007JCLI1824.1.

Roeckner, E., and Coauthors, 2003: The atmospheric general circulation model ECHAM5: Part 1: Model description. Max Planck Institute for Meteorology Rep. 349, 127 pp. [Available online at http://mms.dkrz.de/pdf/klimadaten/service_support/documents/mpi_report_349.pdf.]

Saravanan, R., 1998: Atmospheric low-frequency variability and its relationship to midlatitude SST variability: Studies using the NCAR climate system model. *J. Climate*, **11**, 1386–1404, doi:10.1175/1520-0442(1998)011<1386:ALFVAI>2.0.CO;2.

Sardeshmukh, P. D., and B. J. Hoskins, 1988: The generation of global rotational flow by steady idealized tropical divergence. *J. Atmos. Sci.*, **45**, 1228–1251, doi:10.1175/1520-0469(1988)045<1228:TGOGRF>2.0.CO;2.

Smirnov, D., M. Newman, M. A. Alexander, Y.-O. Kwon, and C. Frankignoul, 2015: Investigating the local atmospheric response to a realistic shift in the Oyashio sea surface temperature front. *J. Climate*, **28**, 1126–1147, doi:10.1175/JCLI-D-14-00285.1.

Taguchi, B., H. Nakamura, M. Nonaka, and S.-P. Xie, 2009: Influences of the Kuroshio/Oyashio Extensions on air–sea heat exchanges and storm-track activity as revealed in regional atmospheric model simulations for the 2003/04 cold season. *J. Climate*, **22**, 6536–6560, doi:10.1175/2009JCLI2910.1.

——, ——, ——, N. Komori, A. Kuwano-Yoshida, K. Takaya, and A. Goto, 2012: Seasonal evolutions of atmospheric response to decadal SST anomalies in the North Pacific subarctic frontal zone: Observations and a coupled model simulation. *J. Climate*, **25**, 111–139, doi:10.1175/JCLI-D-11-00046.1.

Ting, M., and S. Peng, 1995: Dynamics of the early and middle winter atmospheric responses to the northwest Atlantic SST anomalies. *J. Climate*, **8**, 2239–2254, doi:10.1175/1520-0442(1995)008<2239:DOTEAM>2.0.CO;2.

Wen, N., Z. Liu, Q. Liu, and C. Frankignoul, 2010: Observed atmospheric responses to global SST variability modes: A unified assessment using GEFA. *J. Climate*, **23**, 1739–1759, doi:10.1175/2009JCLI3027.1.

Wu, L., and Coauthors, 2012: Enhanced warming over the global subtropical western boundary currents. *Nat. Climate Change*, **2**, 161–166, doi:10.1038/nclimate1353.

Yin, J. H., 2005: A consistent poleward shift of the storm tracks in simulations of 21st century climate. *Geophys. Res. Lett.*, **32**, L18701, doi:10.1029/2005GL023684.

Zhong, Y., and Z. Liu, 2008: A joint statistical and dynamical assessment of atmospheric response to North Pacific oceanic variability in CCSM3. *J. Climate*, **21**, 6044–6051, doi:10.1175/2008JCLI2195.1.

Zhou, G., M. Latif, R. J. Greatbatch, and W. Park, 2015: Atmospheric response to the North Pacific enabled by daily sea surface temperature variability. *Geophys. Res. Lett.*, **42**, 7732–7739, doi:10.1002/2015GL065356.